Temporal precision of the encoding of motion information by visual interneurons

Anne-Kathrin Warzecha, Jutta Kretzberg and Martin Egelhaaf

Background: There is much controversy about the timescale on which neurons process and transmit information. On the one hand, a vast amount of information can be processed by the nervous system if the precise timing of individual spikes on a millisecond timescale is important. On the other hand, neuronal responses to identical stimuli often vary considerably and stochastic response fluctuations can exceed the mean response amplitude. Here, we examined the timescale on which neural responses could be locked to visual motion stimuli.

Results: Spikes of motion-sensitive neurons in the visual system of the blowfly are time-locked to visual motion with a precision in the range of several tens of milliseconds. Nevertheless, different motion-sensitive neurons with largely overlapping receptive fields generate a large proportion of spikes almost synchronously. This precision is brought about by stochastic rather than by motion-induced membrane-potential fluctuations elicited by the common peripheral input. The stochastic membrane-potential fluctuations contain more power at frequencies above 30–40 Hz than the motion-induced potential changes. A model of spike generation indicates that such fast membrane-potential changes are a major determinant of the precise timing of spikes.

Conclusions: The timing of spikes in neurons of the motion pathway of the blowfly is controlled on a millisecond timescale by fast membrane-potential fluctuations. Despite this precision, spikes do not lock to motion stimuli on this timescale because visual motion does not induce sufficiently rapid changes in the membrane potential.

Address: Lehrstuhl für Neurobiologie, Fakultät für Biologie, Universität Bielefeld, Postfach 10 01 31, D-33501 Bielefeld, Germany.

Correspondence: Anne-Kathrin Warzecha
E-mail: ak.warzecha@biologie.uni-bielefeld.de

Background

All information represented by the brain about the outside world is somehow encoded in the electrical activity of nerve cells. As action potentials are perceived as all-or-nothing events, there is a general agreement that most information is contained in their temporal sequence. The question regarding on which timescale the relevant information is encoded is still under debate, however. On the one hand, the precise timing of individual action potentials might be important or, on the other hand, relevant information might simply be conveyed by the mean spike rate within some extended time interval [1–5]. Obviously, the first possibility offers a large information capacity. Indeed, in various types of visual interneurons, sensory information has been concluded to be represented accurately on a millisecond timescale [6–8]. The accuracy of the representation of sensory information by nerve cells on a fine timescale is limited by stochastic sources which lead to variability in neuronal responses. Individual responses of visual interneurons often have variances up to the order of the mean response amplitude [9–12]. From this perspective, it is hard to imagine that neurons operate with a temporal precision in the range of milliseconds.

Here, we have investigated the timescale on which neural responses can be locked to sensory stimuli. In contrast to most previous studies on the reliability of neural coding, we have accounted for the fact that the timing of action potentials is constrained by the biophysical properties of nerve cells. In particular, slow changes in membrane potential are less effective than fast ones in eliciting action potentials (for example, see [13]). Hence, spikes are expected to be precisely time-locked only to sufficiently fast synaptic input.

Our experimental analysis was performed on specific motion-sensitive neurons in the visual system of the fly (for review, see [14,15]). In the fly, certain aspects of neuronal reliability have been investigated at several levels of information processing, ranging from the photoreceptors and their postsynaptic elements to neurons in the main centre of motion computation (the posterior part of the third visual neuropile) [5,8,12,16–22]. In this area of the brain, about 60 so-called tangential neurons use their extended dendrites to pool the signals of many local excitatory and inhibitory motion-sensitive nerve cells which have opposite preferred directions [14,15,23]. Tangential

neurons respond to motion within large parts of the visual field. The various tangential cells differ in their preferred direction of motion, in their receptive field properties and in their response mode. Some of them generate regular spikes, some respond with graded changes of their membrane potential and others respond mainly in the graded fashion but also exhibit small spike-like depolarisations [24–26]. Here, we used several tangential neurons in electrophysiological experiments to investigate the timescale on which action potentials are locked to visual motion and the constraints that limit the accuracy of their timing.
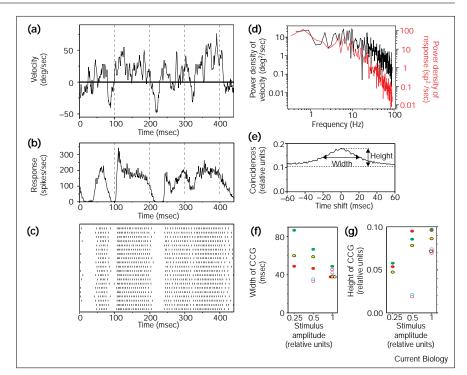
Results

Time-locking of responses to motion stimuli

The question of how well the spike activity of one of the tangential cells, the H1 neuron, is time-locked to time-varying visual motion was investigated by presenting motion stimuli with a randomly modulated velocity. For part of the experiments, a constant velocity baseline was superimposed on these motion stimuli (Figure 1a) in order to increase the overall neuronal activity. The amplitude spectrum of the motion stimulus (Figure 1d) covered large

parts of the complete dynamic range of motion stimuli that is encountered by the fly in natural situations. By deducing the average of many individual response traces, the motion-induced response component was obtained (Figure 1b). The motion-induced response component strongly modulates with the pattern motion, occasionally reaching momentary peak frequencies of more than 300 spikes per second. With respect to these peak activities and to the strongly modulated activity profile, the motion-induced response component appears to be quite similar to that published in another study on the H1 cell [8]. The H1 cell is excited by back-to-front motion, its preferred direction, and inhibited during front-to-back motion, its null direction. Since the spontaneous activity of the H1 neuron is low, the cell stops firing when the pattern moves in the null direction. As a consequence of inevitable time constants of the processes underlying motion computation (reviewed in [23,27]), the power spectrum of the motion-induced response component of the H1 neuron tails off earlier than that of the motion stimulus (Figure 1d). Nevertheless, the time-dependent response of the H1 cell is coupled to visual motion — at

Figure 1

Time-locking of responses of the H1 cell to motion stimuli. **(a)** Section of a motion trace with random velocity fluctuations superimposed on a constant velocity baseline in the cells preferred direction. Positive velocities indicate back-to-front motion and negative velocities indicate front-to-back motion. **(b)** Spike frequency histogram obtained from the responses of four H1 cells to repetitive presentation of the motion trace shown in (a). For each of the four neurons, between 100 and 450 individual responses were averaged. The responses were shifted by 30 msec to compensate for the latency between stimulus and responses. The temporal resolution was 1.1 msec. **(c)** Subsequent sample traces of individual responses of one of the four H1 cells to repetitive stimulation with the same motion trace are plotted underneath each other. The section of the responses shown in (c) corresponds to the section of the spike frequency histogram shown in (b). The time of occurrence of individual spikes is indicated by small vertical bars. **(d)** The black line corresponds to the power spectrum of the velocity trace, a section of which is illustrated in (a). The red line represents the average power spectrum of the motion-induced response components of four H1 cells. **(e)** Averaged cross-correlogram (CCG) between 100 pairs of individual response traces of one H1 cell. Pairs were chosen pseudorandomly ensuring that every individual response trace was used and that no trace was correlated with itself. An ordinate value of 1 indicates that subsequent responses are identical at a temporal resolution of 1.1 msec. The CCG was quantified by determining the height above the level of random activity (dashed lines) and the width at half-maximum height above this level.

For this analysis, all possible combinations of individual response traces were taken into account excluding autocorrelations. The time interval evaluated for the correlograms started 221 msec after the onset of motion and lasted for 2709 msec. The mean spike activity within this interval was 94 spikes/sec. The width and height of CCGs for different cells and stimulus conditions are shown in **(f)** and **(g)**,

respectively. Open symbols correspond to randomly modulated velocity fluctuations that were superimposed on a constant velocity baseline, and closed symbols correspond to fluctuations that were not superimposed. Symbols of the same colour correspond to data obtained from the same cell and animal. Between 100 and 450 individual response traces were evaluated for each CCG.

least on a coarse timescale. This coupling is also obvious from the individual response traces (Figure 1c). Despite some variability in the temporal fine structure of the individual responses, the overall pattern of spike activity looks rather similar in each of the individual responses elicited by identical motion stimulation.
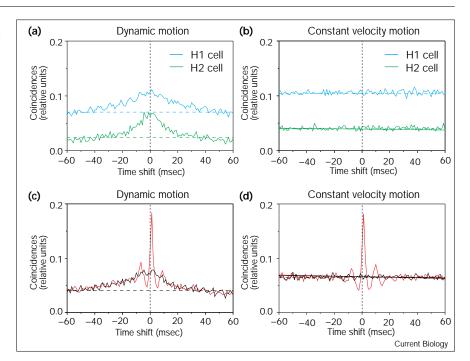
To quantify the similarity of the individual responses and thus their time-locking to the stimulus, the individual response traces were cross-correlated with each other. If there were no jitter in the timing of action potentials across trials and the spikes were precisely locked to the stimulus on a millisecond timescale, the cross-correlogram (CCG) should exhibit a sharp peak at time zero with an amplitude close to 1 when normalised to the height of the corresponding autocorrelograms. In Figure 1e, a normalised sample CCG is shown and this is characterised by a rather broad peak around time zero. The width and height of this peak were quantified by relating the CCG of the individual response traces to the CCG of the responses of a hypothetical, randomly firing neuron with the same mean spike rate. Of course, the latter CCG is entirely flat (Figure 1e). The height of the CCG of the neuronal responses in Figure 1e above the level of random activity amounts to 0.074. The width of the CCG is determined at half-maximum height above the random level and is 42.2 milliseconds for the

example shown in Figure 1e. The width and the height of the CCG depend on whether or not a constant velocity baseline was superimposed on the random motion stimulus, but they never decreased below 30 milliseconds or increased above 0.1, respectively, for the stimulus conditions tested here (Figure 1f,g). Hence, most spikes generated by the H1 neuron are not precisely locked to visual motion on a millisecond timescale. A similar conclusion can be drawn for another spiking tangential neuron of the fly, the H2 cell, as shown in Figure 2a, although here the width of the CCG is somewhat smaller than that obtained for the H1 neuron (animal 1, under contrast condition II / animal 2, under contrast condition I: random motion without superimposed constant velocity — H2 cell, width 18.9/30 msec, height 0.038/0.063, H1 cell, width 38.9/52.2 msec, height 0.043/0.051; random motion with superimposed constant velocity — H2 cell, width 16.7/21.1 msec, height 0.046/0.053, H1 cell, width 35.6/37.8 msec, height 0.036/0.029). In any case, spikes of either tangential neuron are locked to motion stimuli on a timescale of several tens of milliseconds.

Both measurements of the precision with which spikes are time-locked to visual motion, that is the width and the height of the CCG, depend on the dynamics of the motion stimulus. When the velocity is constant, the CCG of the

Figure 2

Synchronisation of spikes in neurons with common synaptic input. Dashed horizontal lines indicate the expected CCG for a neuron firing randomly at the same rate as the respective measured cell(s). Dashed vertical lines indicate a time shift of 0 msec. (a,b) CCGs of pairs of individual response traces of either the H1 cell (blue line) or the H2 cell (green line) to (a) random velocity fluctuations and (b) constant velocity motion. (c,d) CCGs between the simultaneously recorded responses of the H1 and H2 neuron (red lines) and shuffled CCGs of the same number of pseudorandomly chosen H1 and H2 responses that were not recorded simultaneously but obtained from repetitive stimulation with the same motion trace (black lines). The responses to (c) random velocity fluctuations and (d) constant velocity motion are shown. CCGs were normalised to the square root of the product of the peak values in the autocorrelograms of the H1 and H2 cell. An ordinate value of 1 indicates that the responses of both cells are identical at a temporal resolution of 1.1 msec. This value cannot be reached, even if all spikes of the H2 cell were to coincide with a spike of the H1 cell because the H2 cell fires less frequently than the H1 cell. (a,c) The time interval evaluated for the CCGs started 162 msec after the onset of motion and lasted for 3104 msec. The mean spike activity within this interval was 63.3 spikes/sec for the H1 cell and 20.5 spikes/sec for the H2 cell: 30 individual response traces of both cells

were evaluated. Contrast condition II was used in this experiment. (b,d) The time interval evaluated for the CCGs started 1666 msec after the onset of motion and lasted for 1600 msec. The mean spike activity within this interval was 94.5 spikes/sec for the H1 cell and 35.8 spikes/sec for the H2 cell: 60 individual response traces of both cells were evaluated. Contrast condition I was used in this experiment.

corresponding responses is basically flat on the timescale analysed here for both the H1 and the H2 cell (Figure 2b). Accordingly, when the amplitudes of the random velocity fluctuations are reduced, the width of the CCG of the corresponding responses tends to increase and its height decreases (Figure 1f,g). Hence, increasingly less action potentials are time-locked to the motion stimulus if the velocity changes get smaller. Much larger stimulus amplitudes and a larger frequency range than those used here could not be tested with our present stimulation equipment (see Materials and methods). Nonetheless, there are likely to be few instances in the normal world where visual motion encompasses a wider dynamic range than that which could be tested here. Hence, visual motion transients in a behaviourally relevant range affect the timing of action potentials essentially on a timescale of several tens of milliseconds.

Synchronisation of spikes in neurons with common synaptic input

The jitter in the timing of spikes of tangential neurons is not due to inaccuracies of the spike generation mechanism. This conclusion can be drawn from experiments in which the spike activity of two tangential neurons, the H1 and the H2 cell, is monitored simultaneously. Both neurons have largely overlapping receptive fields and the same preferred direction of motion. The H1 and H2 cell are thought to share large parts of their local motion-sensitive input elements and not to be synaptically coupled to each other [28]. The mean activity of the H2 cell is smaller than that of the H1 cell. If the temporal jitter of spikes were primarily caused by noise originating in the common pathway peripheral to the two cells or in the stochastic nature of light rather than by noise intrinsic to the spike generation mechanism itself, most H2 spikes should coincide with an H1 spike. Indeed, the CCG of simultaneously recorded responses of the two neurons to white-noise velocity modulations superimposed on a constant velocity baseline reveals a narrow peak (Figure 2c) with a width of 2.2 milliseconds and a height of 0.14 above the level expected from random spike occurrence. The peak is slightly shifted indicating that the H1 spikes tend to precede spikes of the H2 neuron by about 1.1 milliseconds. The same width of the CCG was obtained for white-noise velocity modulations with and without superimposed constant velocity in a different animal (data not shown). The narrow peak indicates that a large proportion of the spikes of both neurons occur almost synchronously: 31.8% of H2 spikes are generated precisely 1.1 milliseconds after an H1 spike and, thus, virtually synchronously. Only 7% of such near-coincidences are expected if both cells were generating action potentials randomly.

As the mean spike activity of the H1 neuron is about three times larger than that of the H2 neuron, most H1 spikes do not have a counterpart in the H2 cell, which leads to a rather high baseline level of the CCG and,

owing to the normalisation procedure used (see legend of Figure 2), to a peak amplitude of only 0.18. Obviously, the H1 and H2 neurons are able to generate spikes with a great temporal precision, despite the fact that their spikes are not as tightly coupled to the stimulus. The latter conclusion is corroborated by the shuffled CCG of H1 and H2 responses elicited with the same stimulus but not recorded simultaneously. This shuffled CCG has a width of 28.9 milliseconds and a height of 0.036 (Figure 2c). Similar values were obtained for another H1–H2 pair (width: 32.2 msec; height: 0.033). The width of the shuffled CCG thus falls between the widths of the CCGs obtained from the responses of either neuron alone (compare with Figure 2a). As the near-synchronicity of spikes is not induced by the velocity fluctuations of the motion stimuli, we conclude that the origin of this near-synchronicity is either in a common noise source in the peripheral motion pathway of the cells or in the stochastic nature of light. This conclusion is further corroborated by simultaneous recordings from the H1 and H2 cell during stimulation with constant-velocity motion. The CCG of the simultaneously recorded activity reveals a similar peak as obtained for transient motion stimulation (width: 1.1 msec; height: 0.117; Figure 2d), whereas the shuffled CCG is flat (Figure 2d). A CCG of the simultaneously recorded activity of similar width (1.1 msec, 1.1 msec, 2.2 msec) and height (0.109, 0.092, 0.084) was obtained in three other H1–H2 pairs stimulated with constant velocity motion. Essentially the same result was obtained for the resting activity of both neurons (data not shown).
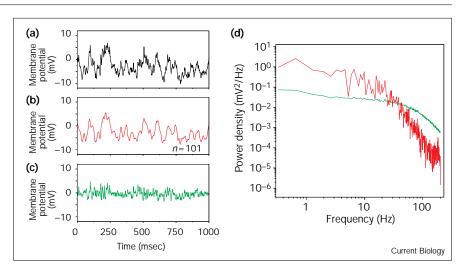
Dynamical properties of the motion-induced and the stochastic response component

As concluded above, the timing of spikes on a millisecond scale is due to stochastic rather than to motion-induced membrane-potential fluctuations. Since the timing of spikes is mainly determined by the membrane potential and its temporal changes at the spike initiation zone, the motion-induced and stochastic fluctuations in the postsynaptic membrane potential can be expected to differ from each other. Therefore, we determined the dynamic properties of the motion-induced and stochastic fluctuations of the postsynaptic membrane potential. In spiking tangential neurons, however, the postsynaptic membrane potential elicited by the motion-sensitive input elements cannot be easily derived from intracellular recordings, because the postsynaptic potentials are superimposed by spikes. Fortunately, there are other tangential neurons in which the postsynaptic membrane-potential changes are much less affected by active membrane processes. These cells can be used to characterise, to a first approximation, the postsynaptic potentials elicited by motion-sensitive input elements.

The HS cells are one class of these cells [25,29] and respond mainly with graded membrane-potential changes

Figure 3

Dynamic properties of the motion-induced and the stochastic response component. The graded membrane-potential changes of an HSN cell, one of the HS cells, are used as a model for the synaptically driven postsynaptic potentials of spiking neurons. The resting potential of the HSN cell was −53.4 mV. **(a)** Section of a sample record of an individual response trace. **(b)** Motion-induced response component as obtained from averaging the responses to 101 presentations of the same motion trace. **(c)** Sample trace of the stochastic response component as obtained from the differences between the motion-induced response component shown in (b) and the single response shown in (a). **(d)** Power spectrum of the stochastic response component averaged over 101 individual power spectra (green line) and power spectrum of the motion-induced response component (red line). The time interval evaluated for the power spectra started 77 msec after the onset of motion and lasted for 3034 msec.

which may be superimposed by only small spike-like depolarisations. The receptive fields of the HS cells largely overlap with those of the H1 and H2 cell. As a consequence, the CCG of the graded membrane-potential changes in the HS cell and the spike response of the H1 cell shows a pronounced peak. Since HS cells are hyperpolarised by motion which leads to an excitation in the H1 cell, the CCG has a negative peak (A-K.W., unpublished observations). The motion-induced response components of the H1 cell and the HS cell induced by random motion stimuli have similar power spectra (compare Figure 1d with Figure 3d). Because of these properties, HS cells are well suited for characterising the synaptically-induced membrane-potential fluctuations.
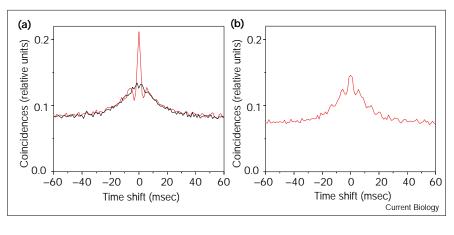
White-noise velocity fluctuations (Figure 3a) were used to determine the dynamic response properties of the post-synaptic potentials elicited in one of the HS cells, the HSN cell. The difference between a single response trace and the motion-induced response component yields the stochastic response component of the respective response trace (Figure 3a–c). The dynamic properties of the stochastic and motion-induced response component are characterised by their power spectra (Figure 3d). The motion-induced response component contains most power at frequencies below 20 Hz. In this frequency range, the power of the motion-induced response component is larger than that of the stochastic response component. Towards higher frequencies, the power of the motion-induced response component steeply decreases. For frequencies above 30–40 Hz, the stochastic response component contains more power than the motion-induced component. Similar power spectra were obtained in two other HS cells as well as in a previous study [30]. As the

noise power is larger than the power of the motion-induced membrane-potential fluctuations at high frequencies, we suggest that these high-frequency stochastic fluctuations are responsible for spike synchronisation in tangential neurons with overlapping receptive fields.
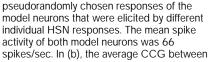
Model simulations of the timing of spikes

Simulations were used to test whether the difference in the dynamics of motion-induced and stochastic membrane-potential fluctuations is the relevant determinant for spike generation. A phenomenological model of the timing of spikes [31,32] was adapted to the spike statistics of the fly tangential neurons (J.K., unpublished observations). The model transforms membrane-potential fluctuations into a sequence of spikes, depending on parameters such as the firing threshold or the refractory time. To account for the stochastic properties of the spike generation mechanism, a noise source is inherent in the model. The membrane-potential fluctuations of the HS cell were used as input signals for a pair of model neurons, and the spike activity of these neurons was simulated. We then examined, in a similar way as for the H1 and H2 cells, under which conditions these model neurons generate action potentials synchronously: we did not intend to mimic the experimentally determined responses quantitatively. The responses of the HS cell were inverted, because it has the opposite preferred direction to the H1 and H2 cell. This procedure allowed us to obtain a good estimate of the post-synaptic potential elicited in the tangential cells by their presynaptic input elements without distortions due to superimposed active processes intrinsic to the HS neuron. When the same individual response trace of the HS cell was inverted and fed into the two model neurons, the CCG of the resulting spike trains displays a pronounced

Figure 4

Model simulations of the timing of spikes. Either **(a)** the individual or **(b)** the motion-induced membrane-potential fluctuations of the HSN cell were inverted and fed into the model for spike generation that transforms its input signals into a sequence of spikes (see Materials and methods). This procedure was performed for two model neurons in order to evaluate how well their spike activity coincided. For each CCG, 99 responses of each model neuron were simulated and cross-correlated. The noise inherent in the simulated spike generation mechanism was different for the two model neurons and for each simulated response but had the same statistical properties. The duration of the simulated spike responses lasted for 2842 msec. The temporal resolution of CCGs was 1.1 msec. In (a), the red line corresponds to the average CCG between simulated spike responses of two model neurons that receive the same intracellularly recorded membrane-potential fluctuations as input signals. The black line corresponds to the shuffled CCG of

Current Biology

pseudorandomly chosen responses of the model neurons that were elicited by different individual HSN responses. The mean spike activity of both model neurons was 66 spikes/sec. In (b), the average CCG between

simulated responses of two model neurons that each received the motion-induced response component as input signal is shown. The mean spike activity of both model neurons was 61 spikes/sec.

peak (Figure 4a). Thus, spike activity in the two model neurons is to a large extent synchronous, similar to that found in real neurons which receive common input. If different individual response traces were fed into the two model neurons, there was no such peak (Figure 4a). Instead, the CCG was similar to the shuffled CCG in Figure 2c. Hence, the stochastic membrane-potential fluctuations in the common input of the model neurons rather than the motion-induced membrane-potential fluctuations are able to synchronise the spikes.

Instead of feeding individual response traces into the model for spike generation, it is also possible to use the motion-induced response component as an input signal in order to find out whether the motion-induced membrane-potential fluctuations contain sufficiently high frequencies to elicit synchronous spikes in pairs of simulated tangential neurons. The CCG of the simulated spike trains resulting from the motion-induced response component has a much smaller and broader peak around time zero (Figure 4b) than that resulting from the corresponding individual response traces (Figure 4a). This result corroborates our conclusion that the differences in the dynamic properties of the motion-induced and the stochastic membrane-potential fluctuations are the reason why most spikes are not locked to motion stimuli on a millisecond timescale.

Discussion
The frequency of action potentials of the directionally selective motion-sensitive tangential cells in the motion pathway of the fly is modulated by velocity changes of moving stimulus patterns. These modulations in spike frequency provide reliable information about pattern motion

on a timescale of several tens of milliseconds. The exact timing of spikes on a millisecond scale is mainly determined by fast stochastic membrane-potential fluctuations. The intrinsic noise in spiking tangential cells is sufficiently small to allow action potentials to time-lock to stochastic membrane-potential fluctuations mediated by the synaptic input of the cell.

The accuracy by which action potentials are time-locked to sensory stimuli depends on at least three constraints, which will be discussed below: the biophysical mechanisms underlying the generation of action potentials; the computations performed in the neuronal pathway from the receptors up to the neuron under consideration; and the properties of neuronal noise.

Constraints imposed by the biophysical mechanisms underlying spike generation
Action potentials are elicited more efficiently by rapid depolarisations than by slow membrane-potential changes. This well-known feature is a consequence of the activation and inactivation kinetics and of the voltage dependence of the ionic conductances underlying action potentials (for example, see [13]). Hence, action potentials are expected to be precisely locked to membrane-potential fluctuations on a millisecond timescale only when these fluctuations are sufficiently fast. Indeed, the occurrence of spikes was found to be tightly time-locked to fluctuations of intracellularly injected current, if this current contained frequencies above approximately 30 Hz [33–35]. Since motion-induced membrane-potential fluctuations in fly tangential neurons elicited by white-noise motion stimuli have less power at frequencies above

30–40 Hz than stochastic membrane-potential fluctuations, these results support our conclusion that most motion-induced membrane-potential fluctuations do not elicit spikes with an accuracy in the millisecond range. This conclusion is not meant to suggest that high-frequency membrane-potential changes larger than the noise cannot be elicited by specific visual stimuli in fly motion-sensitive neurons. Preliminary results indicate that, for instance, bright flashes in the entire visual field or instantaneous step-wise displacements of a high-contrast pattern lead to rapid membrane-potential changes and, accordingly, to a precise time-locking of action potentials (B. Kimmerle, personal communication). It should be noted, however, that these non-motion stimuli will rarely be encountered by an animal outside the laboratory. In conclusion, motion stimuli covering a broad frequency range, which comprises virtually all frequencies of biologically relevant motion, are represented reliably only on a timescale in the range of several tens of milliseconds.

Constraints imposed by the computational properties of the motion pathway

Why do the tangential cells not follow with large gain velocity fluctuations above approximately 20 Hz, even though light-adapted photoreceptors have a cut-off frequency of approximately 100 Hz [36,37]? Any motion detection mechanism needs to compare the brightness changes in neighbouring regions of the visual field. This comparison inevitably involves time constants, in order to provide directionally selective responses (for example, see [27]). These time constants determine the operating range of the motion detection system. Although the time constants in the motion pathway of the fly were found to adapt to the prevailing motion stimuli [38–40], they were estimated to lie in the range between tens and hundreds of milliseconds (reviewed in [23]). Consequently, motion-sensitive neurons do not represent high-frequency components in the motion signal, even if these are well transmitted by the photoreceptors. Hence, the temporal precision by which motion-sensitive neurons generate action potentials is largely limited by the dynamic properties of the computations underlying directional selective-motion detection.

Constraints imposed by neuronal noise

The precision of encoding motion information by action potentials is affected by the stochastic signal fluctuations that are superimposed on the motion-induced responses. As stochastic membrane-potential fluctuations in fly tangential neurons were found to be larger than the motion-induced membrane-potential fluctuations at frequencies above 30–40 Hz, most action potentials are eventually time-locked on a millisecond scale to stochastic rather than to motion-induced membrane-potential fluctuations. As revealed by the near-synchronicity of action potentials of neurons with largely overlapping receptive fields, these stochastic membrane-potential fluctuations are to a large extent transmitted by the local motion-sensitive input elements of the spiking tangential neurons. The mechanisms underlying spike generation in the tangential cells therefore appear to be precise enough to allow this near-synchronicity. This result is in contrast to an earlier notion based on rather indirect evidence [12,41]. Obviously, there are various potential noise sources which may limit the precision with which motion information is encoded. These sources range from the stochastic nature of light to all sorts of biophysical mechanisms that underlie the electrical activity of nerve cells. We are currently investigating the noise sources in the visual system of the fly which are most decisive in limiting the reliability of motion computation.

The finding that spikes in fly tangential cells with greatly overlapping receptive fields are highly synchronised is reminiscent of similar findings in retinal ganglion cells of various vertebrate species [42,43] and the lateral geniculate nucleus of the cat [44]. The synchronisation of spike activity in these systems has been suggested to be significant for solving certain computational tasks. The synchronisation might equally well be a simple by-product of the common synaptic input of the synchronised cells, however.

In related studies on the H1 neuron of the fly [8,30], the variability of neuronal responses to dynamic stimuli has been concluded to be much smaller than the variability of responses to constant stimuli. One of these studies makes this claim without any quantitative analysis [30]. The other study [8] uses the variance of the spike count across trials as a measure of response variability. As the data obtained with constant and with dynamic stimuli were evaluated and plotted in different ways [8], it is hard to compare the corresponding variances. In the plot depicting the variance of the responses to constant velocity stimuli, the spike count was increased in two ways, that is by increasing the stimulus velocity and by increasing the time windows within which spikes were counted. By contrast, in the plots showing the variance for the dynamic stimuli the time window was constant, so that variations of the spike count are only due to the velocity changes inherent in the dynamic stimuli. If only those data points which were presumably determined with the same counting window are compared, it is obvious that the variances of the responses to constant and dynamic stimuli differ by less than an order of magnitude. We are currently investigating whether these small differences between two single experiments turn out to be significant. First results indicate that the variances obtained for constant and dynamic motion stimuli are very similar when both types of stimuli are alternately presented to the same fly (A-K.W. and M.E., unpublished observations).

A much more precise time-locking of spikes to stimuli than in the motion pathway of the fly is found for other sensory modalities, such as the electrosensory system of

certain species of fish [45], the auditory system of vertebrates [46] and the mechanosensory system of the fly [47]. The stimulus-induced membrane-potential changes in these systems are much faster than those in motion vision systems and resolve stimulus frequencies up to several hundred Hz. It should be noted that, in these other systems, extremely precise time-locking of spikes to the sensory input is a basic requirement for solving the respective computational tasks of these systems. In contrast to these systems, there might be no computational requirements for precise time-locking of spikes to visual motion stimuli. Biological motion vision systems are required either to sense objects moving in the animal's visual field or to sense the animal's self-motion. In either case, behaviourally relevant motion stimuli might hardly change their direction at frequencies that would demand a temporal precision in the millisecond range. Whether this notion is true needs to be elucidated in experiments in which the dynamics of the natural motion input of animals is analysed. At least in the fly, first attempts have been made in this respect by analysing the coding of motion stimuli that were generated in a flight simulator by the fly's own actions and reactions. In the context of optomotor course stabilisation, the resulting velocity fluctuations had most power at frequencies below 5 Hz [48]. Accordingly, on the basis of the H1 neuron response, these behaviourally generated motion stimuli can be decoded most reliably at a timescale of some tens of milliseconds, that is on a timescale in which the timing of individual spikes does not matter [22]. Even when male flies virtuosically chase females in the context of mating behaviour, only up to ten changes of direction of the animal's path of flight per second are observed [49,50]. Hence, it might not be a disadvantage for an animal to have a motion pathway that does not represent stimuli with a precision in the millisecond range.

Conclusions

Motion-sensitive neurons in the fly are capable of signalling presynaptic events by the timing of their spikes with a temporal precision in the order of a millisecond, but only if the presynaptic signals are sufficiently transient. Most spikes are not locked to motion stimuli with a temporal precision in the millisecond range because, as a consequence of the computations underlying motion detection, the membrane-potential fluctuations induced by visual motion are usually not fast enough. Instead, the timing of most spikes on a fine timescale is determined by stochastic signal fluctuations mediated by the presynaptic elements of the motion-sensitive neuron. Even if the velocity fluctuations are very fast, the spike activity is modulated by visual motion only on a less fine timescale. As motion detection in most animals underlies similar computational constraints, it is expected that the precision of spike timing is similar in other motion–vision systems.

Materials and methods
Preparation and electrophysiology
Experiments were performed on 1–8 day old female blowflies (*Calliphora erythrocephala*). Animals were dissected as described previously [51]. The experiments were performed at temperatures between 20 and 25°C. The probed tangential neurons could be identified individually by the location and size of their receptive fields as well as the shape of their signals and preferred direction of motion. The spike activity of the H1 and H2 neurons, which have similar receptive fields and the same preferred direction of motion, were recorded from their respective telodendrons which reside in different parts of the brain [28]. Action potentials from these two neurons were recorded extracellularly. The HS neurons that respond mainly with graded changes of their membrane potential were recorded intracellularly. For extracellular recordings, either tungsten electrodes or glass capillaries filled with 1 M KCl were used. The electrodes had resistances ranging from 3 to 10 MΩ. For intracellular recording, glass micropipettes (Clark Electromedical) were pulled on a Brown-Flaming puller (Sutter Instruments). The micropipettes were filled with 1 M KCl and had resistances between 40 and 80 MΩ. Recorded signals were monitored by standard electrophysiological equipment. The noise band of intracellular electrodes was at least two orders of magnitude smaller than the smallest response component. Extracellularly recorded spikes were converted into pulses of fixed amplitude and duration. Signals were fed into a 486-PC through an AD-converter of an I/O card (Data Translation) at a rate of 900 Hz (Figure 2) or 2700 Hz (all other experiments). For comparison of the CCGs, responses sampled at 2700 Hz were reduced to an elementary time bin of 1.1 msec before further data evaluation. The programs for data acquisition and evaluation as well as for the control of stimulus movements were written in ASYST (Keithley Instruments).

Visual stimulation
For visual stimulation, a vertically oriented square-wave grating was generated on a monitor (Tektronix 608) by an image synthesiser (Picasso) at a frame rate of 183 Hz. The position of the grating was controlled via the image synthesiser by a PC. The horizontal and vertical angular extent of the screen ranged from 15°–77° and from −24° to +24°, respectively, with 0° referring to the frontal midline of the animal. The monitor screen was oriented perpendicular to the horizontal plane of the animal's head. Pattern wavelength amounted to either 7.8° (Figure 2) or 6.2° (all other experiments). The mean luminance and contrast was either 4 cd/m^2 and 95% (termed contrast condition I) or 49 cd/m^2 and 45% (termed contrast condition II). If not otherwise specified, contrast condition I was used. During the experiments the grating moved either at a constant temporal frequency of 4 Hz (Figure 2b,d) or with white-noise velocity fluctuations that were modulated randomly according to a Gaussian distribution with a standard deviation of 0.122° (Figure 2a,c) or 0.097° (Figures 1,3) per time bin. For the responses obtained with an acquisition rate of 900 Hz, stimulus control and data acquisition could be achieved by the same PC. The time bin thus amounted to 1.1 msec. For the other experiments in which data were sampled at a higher frequency, two PCs were used for data acquisition and stimulus control. In these experiments, the time bin for stimulus control was 0.56 ms. In part of the experiments the random velocity fluctuations were superimposed by a constant velocity with a temporal frequency of 2 Hz in the preferred direction of the H1 and H2 cell and thus in the null direction of the HS cells. Despite the fast output modulations of the signal controlling the pattern velocity, the frame rate of the image synthesiser was considerably slower (i.e. 183 Hz), thus limiting the dynamic range of the motion stimuli. To be able to characterise the frequency content of the stimulus, the velocity trace was lowpass-filtered with a cut-off at 80 Hz for the experiments in which the time-locking on different stimuli was investigated systematically (Figure 1). This procedure did not much affect the neuronal responses (compare Figure 1e–g with Figure 2a and Figure 1d with Figure 3d). The luminance modulations as well as the elementary pattern displacements introduced by the display of each new frame did not induce a pronounced time-locking of the responses: the peak in the power spectrum of Figure 3d at 183 Hz is only rather small and at most half as large as the corresponding stochastic response component at the same frequency. This shows that the stimuli employed in the

present study are a good approximation to 'smooth' motion. The experimental protocol consisted of a series of consecutive sweeps. At the beginning of each sweep, the data acquisition was triggered by the frame synchronisation signal of the image synthesiser. It was ensured that at the end of each sweep data acquisition and stimulus control were still synchronised within 1.1 msec for the experiments illustrated in Figure 2 and 0.7 msec for all other experiments. Between consecutive presentations the stimulus pattern was stationary for about 2 sec. The spatial phase of the stimulus was identical for each stimulus presentation. Neuronal responses were recorded for 4.1 sec (4.4 sec for experiment shown in Figure 2) starting 1 sec (1.1 sec) before the onset of motion.

Model simulations
Spike generation was modelled by the following procedure modified from Gerstner [31,32]. For each elementary time step, the following procedure was employed. The actual threshold for spike generation was calculated, the spike propability was determined, and it was decided whether a spike was generated or not.

The threshold of the membrane potential at which a spike is elicited, $\theta(t)$, was calculated for the actual instance in time, t. It was assumed that the spike threshold depends on the time, s, elapsed after the last action potential. With an absolute refractory time, γ_{ref}, the threshold was modelled according to the following formula:

$$\theta(t) = \begin{cases} \infty & \text{for } s \le \gamma_{ref} \\ \theta_0 + \frac{\eta}{s - \gamma_{ref}} & \text{for } s > \gamma_{ref} \end{cases} \tag{1}$$

$\theta(t)$ converges towards θ_0 when the last action potential has been generated a long time ago: η determines how fast $\theta(t)$ converges.

In the next step, the probability for a spike, $P(h,\theta)$, was calculated. It depends on the difference between the actual threshold value $\theta(t)$ and the membrane potential h(t): the h(t) value was taken from the inverted intracellular responses of the HS cell. Then the probability for a spike is given by

$$P(h,\theta) = 1 - e^{-\left(\frac{\Delta t}{\tau_0}\right) e^{\beta\left[h(t) - \theta(t)\right]}} \tag{2}$$

with τ_0 being the mean response time for $h = \theta$, β being a weighting factor that determines to what extent the model is affected by noise and Δt being the elementary time step.

Eventually $P(h,\theta)$ was compared to a uniformly distributed random number between 0 and 1. If $P(h,\theta)$ was larger than this random number a spike was generated. In this way a sequence of spikes can be generated for consecutive elementary time steps. Parameters were adjusted to the spike statistics of fly tangential neurons (J.K., unpublished observations).

The parameters used to simulate the spike trains for Figure 4 were: $\theta_0 = 2$ mV (above the resting potential); $\gamma = 0.175$ msec; $\eta = 19.8$ mV•msec; $\tau_0 = 1.5$ msec; $\beta = 1.5$ mV^{-1} ; $\Delta t = 0.37$ msec.

The programs for simulation of the spike generating mechanism were written in NEO, a software package developed by Helge Ritter, Department of Neuroinformatics, University of Bielefeld, Germany.

Acknowledgements

References
1. Perkel DH, Bullock TH: **Neural coding.** *Neurosci Res Progr Bulletin* 1968, **3**:405-527.
2. Shadlen MN, Newsome WT: **Noise, neural codes and cortical organization.** *Curr Opin Neurobiol* 1994, **4**:569-579.
3. Softky WR: **Simple codes versus efficient codes.** *Curr Opin Neurobiol* 1995, **5**:239-247.
4. Shadlen MN, Newsome WT: **Is there a signal in the noise?** *Curr Opin Neurobiol* 1995, **5**:248-250.
5. Rieke F, Warland D, de Ruyter van Steveninck R, Bialek W: *Spikes – Exploring the Neural Code.* Cambridge, Massachusetts: MIT Press; 1997.
6. Bair W, Koch C: **Temporal precision of spike trains in extrastriate cortex of the behaving Macaque monkey.** *Neur Comput* 1996, **8**:1185-1202.
7. Berry MJ, Warland DK, Meister M: **The structure and precision of retinal spike trains.** *Proc Natl Acad Sci USA* 1997, **94**:5411-5416.
8. Ruyter van Steveninck Rd, Lewen GD, Strong SP, Koberle R, Bialek W: **Reproducibility and variability in neural spike trains.** *Science* 1997, **275**:1805-1808.
9. Levine MW, Cleland BG, Zimmerman RP: **Variability of reponses of cat retinal ganglion cells.** *Vis Neurosci* 1992, **8**:277-279.
10. Tolhurst DJ, Movshon JA, Dean AF: **The statistical reliability of signals in single neurons in cat and monkey visual cortex.** *Vis Res* 1983, **23**:775-785.
11. Britten KH, Shadlen MN, Newsome WT, Movshon JA: **Responses of neurons in macaque MT to stochastic motion signals.** *Vis Neurosci* 1993, **10**:1157-1169.
12. Warzecha A-K: **Reliability of neuronal information processing in the motion pathway of the blowflies *Calliphora erythrocephala* and *Lucilia cuprina* [PhD Thesis].** Tübingen: Universität Tübingen; 1994.
13. Johnston D, Wu M-S: *Foundations of Cellular Neurophysiology.* Cambridge, Massachusetts: MIT Press; 1995.
14. Hausen K, Egelhaaf M: **Neural mechanisms of visual course control in insects.** In *Facets of Vision.* Edited by Stavenga D, Hardie R. Berlin. Heidelberg, New York: Springer-Verlag; 1989:391-424.
15. Egelhaaf M, Borst A: **A look into the cockpit of the fly: visual orientation, algorithms, and identified neurons.** *J Neurosci* 1993, **13**:4563-4574.
16. Laughlin SB, Howard J, Blakeslee B: **Synaptic limitations to contrast coding in the retina of the blowfly *Calliphora*.** *Proc R Soc Lond Biol* 1987, **231**:437-467.
17. Laughlin SB, Ruyter van Steveninck Rd: **The rate of information transfer at graded-potential synapses.** *Nature* 1996, **379**:642-645.
18. Juusola M, French AS, Uusitalo RO, Weckström M: **Information processing by graded-potential transmission through tonically active synapses.** *Trends Neurosci* 1996, **19**:292-297.
19. Bialek W, Rieke F, Ruyter van Steveninck Rd, Warland D: **Reading a neural code.** *Science* 1991, **252**:1854-1857.
20. Ruyter van Steveninck Rd, Bialek W: **Real-time performance of a movement-sensitive neuron in the blowfly visual system: coding and information transfer in short spike sequences.** *Proc R Soc Lond Biol* 1988, **234**:379-414.
21. Ruyter van Steveninck Rd, Bialek W: **Reliability and statistical efficiency of a blowfly movement-sensitive neuron.** *Phil Trans R Soc Lond Biol* 1995, **348**:321-340.
22. Warzecha A-K, Egelhaaf M: **How reliably does a neuron in the visual motion pathway of the fly encode behaviourally relevant information?** *Eur J Neurosci* 1997, **9**:1365-1374.
23. Egelhaaf M, Borst A: **Movement detection in arthropods.** In *Visual motion and its role in the stabilization of gaze.* Edited by Wallman J, Miles FA. Amsterdam: Elsevier; 1993:53-77.
24. Hengstenberg R: **Spike responses of 'non-spiking' visual interneurone.** *Nature* 1977, **270**:338-340.
25. Hausen K: **Motion sensitive interneurons in the optomotor system of the fly. I. The Horizontal Cells: structure and signals.** *Biol Cybern* 1982, **45**:143-156.
26. Haag J, Theunissen F, Borst A: **The intrinsic electrophysiological characteristics of fly lobula plate tangential cells: II. Active membrane properties.** *J Computat Neurosci* 1997, **4**:349-369.
27. Borst A, Egelhaaf M: **Principles of visual motion detection.** *Trends Neurosci* 1989, **12**:297-306.
28. Hausen K: **Monocular and binocular computation of motion in the lobula plate of the fly.** *Verh Dtsch Zool Ges* 1981, **74**:49-70.
29. Hausen K: **Motion sensitive interneurons in the optomotor system of the fly. II. The Horizontal Cells: receptive field organization and response characteristics.** *Biol Cybern* 1982, **46**:67-79.
30. Haag J, Borst A: **Encoding of visual motion information and reliability in spiking and graded potential neurons.** *J Neurosci* 1997, **17**:4809-4819.
31. Gerstner W, van Hemmen JL: **Associative memory in a network of 'spiking' neurons.** *Network* 1992, **3**:139-164.
32. Gerstner W: *Reihe Physik, Band 15: Kodierung und Signalübertragung in Neuronalen Systemen.* Frankfurt: Verlag Harri Deutsch; 1993.
33. Mainen ZF, Sejnowski TJ: **Reliability of spike timing in neocortical neurons.** *Science* 1995, **268**:1503-1506.

34. Nowak LG, Sanchez-Vives MV, McCormick DA: **Influence of low and high frequency inputs on spike timing in visual cortical neurons**. *Cerebral Cortex* 1997, **7**:487-501.

35. Haag J, Borst A: **Amplification of high frequency synaptic inputs by active dendritic membrane processes**. *Nature* 1996, **379**:639-641.

36. Laughlin S: **Neural principles in the peripheral visual systems of invertebrates**. In *Handbook of Sensory Physiology,* Vol.VII/6B. Edited by Autrum H. Berlin. Heidelberg, New York: Springer; 1981:133-280.

37. Hardie RC: **Functional organization of the fly retina**. In *Progress in Sensory Physiology 5.* Edited by Autrum H, Ottoson D, Perl ER, Schmidt RF, Shimazu H, Willis WD. Berlin, Heidelberg, New York, Tokyo: Springer; 1985:1-79.

38. Maddess T, Laughlin SB: **Adaptation of the motion-sensitive neuron H1 is generated locally and governed by contrast frequency**. *Proc R Soc Lond Biol* 1985, **225**:251-275.

39. Ruyter van Steveninck Rd, Zaagman WH, Mastebroek HAK: **Adaptation of transient responses of a movement-sensitive neuron in the visual system of the blowfly, *Calliphora erythrocephala***. *Biol Cybern* 1986, **54**:223-236.

40. Borst A, Egelhaaf M: **Temporal modulation of luminance adapts time constant of fly movement detectors**. *Biol Cybern* 1987, **56**:209-215.

41. Warzecha A-K, Egelhaaf M: **Neuronal signal fluctuations limit the coding of motion information in the blowfly *Calliphora***. In *Göttingen Neurobiology Report 1994.* Edited by Elsner N, Breer H. Stuttgart, New York: Georg Thieme Verlag; 1994, 446.

42. Mastronarde DN: **Correlated firing of retinal ganglion cells**. *Trends Neurosci* 1989, **12**:75-80.

43. Meister M: **Multineuronal codes in retinal signaling**. *Proc Natl Acad Sci USA* 1996, **93**:609-614.

44. Alonso J-M, Usrey WM, Reid RC: **Precisely correlated firing in cells of the lateral geniculate nucleus**. *Nature* 1996, **383**:815-819.

45. Kawasaki M: **Temporal hyperacuity in the gymnotiform electric fish, *Eigenmannia***. *Amer Zool* 1993, **33**:86-93.

46. Carr CE: **Processing of temporal information in the brain**. *Annu Rev Neurosci* 1993, **16**:223-243.

47. Fayyazuddin A, Dickinson MH: **Haltere afferents provide direct, electrotonic input to a steering motor neuron in the blowfly, *Calliphora***. *J Neurosci* 1996, **16**:5225-5232.

48. Warzecha A-K, Egelhaaf M: **Intrinsic properties of biological movement detectors prevent the optomotor control system from getting unstable**. *Phil Trans R Soc Lond Biol* 1996, **351**:1579-1591.

49. Wagner H: **Flight performance and visual control of flight of the freely-flying housefly (*Musca domestica* L.) II. Pursuit of targets**. *Phil Trans R Soc Lond Biol* 1986, **312**:553-579.

50. Land MF: **Chasing and pursuit in the dolichopodid fly *Poecilobothrus nobilitatus***. *J Comp Physiol [A]* 1993, **173**:605-613.

51. Warzecha AK, Egelhaaf M, Borst A: **Neural circuit tuning fly visual interneurons to motion of small objects. I. Dissection of the circuit by pharmacological and photoinactivation techniques**. *J Neurophysiol* 1993, **69**:329-339.